Transportation Research Record

Dynamic Weighted Resilience Metrics of Transport Networks: an Approach to Quantify the Impact of Disruptions on Traffic Conditions

--Manuscript Draft--

Full Title:	Dynamic Weighted Resilience Metrics of Transport Networks: an Approach to Quantify the Impact of Disruptions on Traffic Conditions
Abstract:	Transport networks are essential for our societies. Their proper operations has to be preserved to face any perturbation or disruption. Therefore, it is of paramount importance to address the modeling and the quantification of the resilience of such networks to ensure an acceptable level of service (LoS) even in presence of disruptions. The paper aims at characterizing network resilience through weighted degree centrality. To do so, we use a real dataset issued from probe vehicle data to weight the graph by the traffic load. In particular, a set of disrupted situations retrieved from our dataset is analyzed to quantify their impact on network operations. Results demonstrate the ability of the proposed metrics to capture traffic dynamics as well as their utility for quantifying the resilience of the network. The proposed methodology combines different metrics from complex networks theory, i.e., heterogeneity, density and symmetry, computed on temporal and weighted graphs. We analyze their variations with respect to time-varying traffic conditions and disruptions, by providing relevant insights on the network states via 3D-maps.
Manuscript Classifications:	Security and Emergencies; Critical Transportation Infrastructure Resilience and Security ABR10; Risk and Resilience Management; Transportation Systems Resilience and Sustainability ABR00; Resilence and Sustainability A0020; Extreme Weather; Resilience and Sustainability; General
Manuscript Number:	
Article Type:	Presentation and Publication
Order of Authors:	Elise Henry
	Angelo Furno
	Nour-Eddin El Faouzi

Dynamic Weighted Resilience Metrics of Transport Networks: an Approach to Quantify the Impact of Disruptions on Traffic Conditions

Submission Date: August 1st, 2019

Elise Henry[1],
[1] Univ. Lyon, IFSTTAR, ENTPE, LICIT UMR_T9401, F-69675, Lyon, France
elise.henry@ifsttar.fr

Angelo Furno[1],
[1] Univ. Lyon, IFSTTAR, ENTPE, LICIT UMR_T9401, F-69675, Lyon, France
angelo.furno@ifsttar.fr

Nour-Eddin El Faouzi[1,2]
[1] Univ. Lyon, IFSTTAR, ENTPE, LICIT UMR_T9401, F-69675, Lyon, France
[2] Queensland University of Technology, STRC, Gardens Point Campus, 2 George Street, G.P.O. Box 2434, Brisbane, Queensland 4001, Australia.
nour-eddin.elfaouzi@ifsttar.fr

Submitted to the 99th Annual Meeting of the Transportation Research Board for publication and presentation

---

Word Count:

Number of words: 6493
Number of tables: 0 (250 words each)
Number of figures: 6 (6 figures max)
Total: 6493

Abstract

Transport networks are essential for our societies. Their proper operations has to be preserved to face any perturbation or disruption. Therefore, it is of paramount importance to address the modeling and the quantification of the resilience of such networks to ensure an acceptable level of service (LoS) even in presence of disruptions.

The paper aims at characterizing network resilience through weighted degree centrality. To do so, we use a real dataset issued from probe vehicle data to weight the graph by the traffic load. In particular, a set of disrupted situations retrieved from our dataset is analyzed to quantify their impact on network operations.

Results demonstrate the ability of the proposed metrics to capture traffic dynamics as well as their utility for quantifying the resilience of the network. The proposed methodology combines different metrics from complex networks theory, i.e., heterogeneity, density and symmetry, computed on temporal and weighted graphs. We analyze their variations with respect to time-varying traffic conditions and disruptions, by providing relevant insights on the network states via 3D-maps.

Keywords: **Smart Transportation, Resilience, Dynamic Graph, Degree Centrality, Heterogeneity**

1. INTRODUCTION

Transport networks are frequently subject to various types of disruptions: they are vulnerable to extreme weather events and naturally prone to both human attacks and technological failures.

As mobility is essential for our society, guaranteeing and increasing the *resilience* of transport network represents a fundamental challenge in transport research. Resilience is defined as *the ability of a transportation system to move people around in the face of one or more major obstacles to normal function*[1]. The interest is twofold: from one side, transport authorities seek for higher resilience towards implementing more reliable, cost-efficient and maintainable systems; from the other side, travelers benefit from resilience in terms of improved level of service and increased availability of mobility services. Finally, by promptly detecting and even anticipating network reactions in case of disturbances, it becomes possible to rapidly managing emergency situations thus reducing the occurrence of gridlocks, accidents and delays that might cause huge costs in terms of economy and human life.

Nowadays, the resilience is assessed either statically, based on the network topology using the graph theory [1, 2, 3], or dynamically, derived from traffic variables evolution [1, 4, 5]. Because topological approaches are unable to grasp the time-dependent aspects of resilience, it is essential to combine both approaches because of their complementary nature [1, 6, 7]. Most resilience studies traditionally focus on small-scale networks with static conditions. By addressing city-wide scale and by taking into account dynamic information on traffic conditions (made possible by the growing availability of real-time data on users' mobility and network conditions), it becomes possible to achieve an accurate overview of the network state, typically neglected in most studies on transport resilience.

Consequently, this paper aims at investigating novel solutions for resilience modeling and analysis for road transport, by trying to answer the following questions:

- How can we characterize a whole road network in terms of resilience by taking into account both topological and traffic dynamics?
- How can we characterize and quantify the resilience of a whole network at a global scale?

This work seeks therefore to advance the state-of-the-art research in the field of resilience with the following contributions: (1) we analyze the impact of abnormal conditions using degree-related metrics computed over a dynamically-weighted graph that grasp both realistic and time-varying traffic-properties of the considered road network; (2) we characterize network *heterogeneity* in a spatio-temporal way. We observe the impact of disturbance at global scale, per geographical areas and in time, as quantified by three resilience indicators presented in the very recent study of Gao et al. [8], briefly discussed in Sec. 2.

The paper is organized as follow. Section 2 briefly surveys related work dealing with resilience, and, particularly, network heterogeneity. Section 3 outlines the proposed methodology to construct a dynamic weighted graph that could be a relevant representation of a city-wide road network, under both typical and abnormal conditions. Such graph is used as an input to compute network heterogeneity used to define the network resilience. In Section 4, we present our case study and discuss the application of the proposed methodology in a realistic scenario. In Section 5 we conclude our paper by discussing the main insights deriving from our case study and highlighting research directions for future work.

[1] https://rideamigos.com/transportation-resilience/

2. LITERATURE REVIEW

2.1. Resilience approaches

As introduced before, there are two major approaches for the network resilience analysis, often lead separately despite their complementarity.

The dynamic approaches define the network resilience through the dynamics traffic conditions, by quantifying the evolution of demand-sensitive traffic variables, such as the travel time, the queue length or the road capacity, in presence of disruptions. A set of such indicators, allowing to evaluate the impact of a disturbance, have been surveyed in [24]. Jenelius et al. [5] defined two metrics, the importance and the exposure, respectively based on the per-edge rise of travel cost and the expected travel cost increase when a disruption occurs. They are among the most popular metrics that belong to the category of dynamic approaches [1, 5, 6].

Based on graph theory, the topological approaches quantify the network resilience through centrality measures. The betweenness centrality, characterizing the node criticity regarding the number of time the shortest path crossed it, the closeness centrality, informing about how an intersection is to all others reachable through the paths' length, and the degree centrality, later defined, are often used to quantify the resilience of networks are among the preferred ones in resilience analysis [9, 10, 11]. Most centrality measures allow to classify the node or the edge regarding their vulnerability. On the contrary, the global efficiency [12], based on the shortest paths' lengths and quantifying how the information is exchanged over the network, provides a global overview of the network performances. Via this measure, we are able to determine the global impact of a disturbance [1, 13, 14].

Given approaches complementarity, Gauthier et al. [6] proposed to dynamically weight the graph with traffic variables to consider traffic dynamics in centrality measures computations. Indeed, in [15, 7, 16] the edge weight sensitivity of the centrality measures and thus their traffic dynamics consideration is verified. Indeed, in correlation analysis between centrality measures, the betweenness centrality in most of cases, and traffic variables characterized by the traffic flow, the travel time graph weighting allows to increase the coefficient [17, 18, 19].

2.2. Network heterogeneity

The *heterogeneity*, also known as *graph irregularity*, quantifies global network information by describing the diversity of network nodes' connectivity [20]. Computed over a weighted graph, the heterogeneity takes traffic dynamics into account.

The definition of heterogeneity is typically based on degree centrality, used as the local metric to describe nodes' connectivity. Degree centrality measures, per each node of the graph, the number of edges adjacent to the considered node. It can be interpreted as the capacity of a node to directly join another node through the network. On directed graphs, where each edge has a direction, it is possible to distinguish between in-degree and out-degree centrality, using the number of edges entering (resp. exiting) the analyzed node. This metric could also be estimated over a weighted network by computing a weighted degree centrality as in [21, 22, 23, 24, 25]. In the weighted case, the degree centrality of a node corresponds to the sum of all the edge weights connected to it. As with the traditional degree centrality, the weighted one can be extended to in-degree (resp. out-degree) and is equal to the sum of the weights for the edges joining the node i to its predecessors (resp. successors) j.

Snijders [26], Zimmermann et al. [27] and Smith et al. [28] characterize network heterogeneity by using degree variance variants: non-standardized or normalized by the average degree, by the variance of the quasi-star network or by the number of graph components. Similarly, Collatz et al. [29] quantify heterogeneity by comparing the largest eigenvalue of the adjacency matrix with the average degree. Finally, Albertson [30] quantifies graph irregularity as the difference of the degree for all the vertices. According to Albertson's definition of heterogeneity, a graph is homogeneous when all node degrees are equal. Estrada [31], Yousaf et al. [32] slightly modified the definition of heterogeneity by comparing a function of these degrees *clarify what do you mean by "comparing a function".*

Network heterogeneity can also be studied by computing the entropy of the degree distribution $P(k)$. This metric captures the disorder of the analyzed network [33, 34, 35]. According to Wang et al. [36], the metric describes the network's heterogeneity, directly related to the resilience. Indeed, this statistical measure is related to loss of information in a network and thus directly concerned with the information transfer.

To characterize complex networks, such as transport ones, in terms of the diversity of connections, Jacob et al. [20] proposes a new measure of heterogeneity, highly dependent of the degree spectrum rather than degree values. By analyzing the degree distribution of a network, the authors are able to define graph heterogeneity. A graph is considered heterogeneous if all the nodes have a different degree. Thus, a star-network is almost considered homogeneous because only one node has a different degree from all others. Although, realized with an undirected and unweighted network, the study can be extended to the weighted case, by computing a weighted degree and analyzing the in-degree and the out-degree distributions.

Gao et al. [8] also propose a heterogeneity metric, computed over a directed weighted graph, based on the in-degree and out-degree density functions, and defined as follows:

$$h = \frac{\sigma_{in}\sigma_{out}}{\langle k \rangle} \tag{1}$$

where σ_{in}^2 (resp. σ_{out}^2) is the variance of density function of the weighted in-degree $P(k_{in})$ (resp. out-degree $P(k_{out})$) and $\langle k \rangle$ is the average degree or network density, defined as follows:

$$\langle k \rangle = \frac{1}{N}\sum_{i=1}^{N} k_i \tag{2}$$

where N is the number of nodes in the network and k_i is the degree of the node i.

In their work, Gao et al. propose a methodology to quantify the resilience of different types of multi-dimensional systems (i.e., gene regulatory, ecological and power supply networks). The authors prove that resilience properties can be effectively grasped via a combination of network metrics that includes: heterogeneity h, density $\langle k \rangle$ (i.e., average degree (Eq. 2)) and network symmetry S. Symmetry is defined as the correlation coefficient of in-degree and out-degree:

$$S = \frac{\langle k_{in}k_{out}\rangle - \langle k_{in}\rangle\langle k_{out}\rangle}{\sigma_{in}\sigma_{out}} \tag{3}$$

where $\langle k_{in} \rangle$ (resp. $\langle k_{out} \rangle$) is the average in-degree (resp. out-degree), $\langle k_{in}k_{out} \rangle$ the scalar product of both vectors (in-degree and out-degree).

A macroscopic resilience parameter β_{eff} (Eq. 4) is then defined as a function of the aforementioned metrics for bacterial and gene regulatory networks.

$$\beta_{eff} = \langle k \rangle + Sh \tag{4}$$

The β_{eff} coefficient is defined based on the Michaelis-Menten equation [37] that defines the dynamics of regulatory networks. In other words, by defining a function that characterizes the network dynamics, the authors determine the critical transition plane β^c_{eff}, separating the desired resilient state, from the undesired one, i.e., non-resilient. In the transport field, the fundamental diagram define network dynamics by relating the speed and the vehicle concentration. To obtain the same trend than the Michaelis-Menten one, we can relate the free flow speed minus the observed one to the concentration.

In this paper, we advocate that a similar approach can be transposed to transport network. To best of our knowledge, this is the first time a similar methodology is used for transportation resilience analysis and quantification. First, we generate a dynamic weighted graph representing a large-scale, time-varying road network. The graph is obtained by mining a large-scale, real-world dataset reporting GPS observations (position, timestamps and speed) collected by probe vehicles. Atop this graph, we verify and prove that heterogeneity, symmetry and network density are sensitive to demand temporal variations, minor perturbations and extreme weather conditions. Thus, these metrics can be used as valid indicators, and therefore predictors, of network resilience for transport networks when modelled as dynamic weighted graphs.

3. METHODOLOGY

Our analysis aims at analyzing the spatio-temporal evolution of the values of heterogeneity, density and symmetry for a dynamic transport network, i.e., a road network represented as a weighted, directed graph, $G(V, E, W^t)$, whose nodes V correspond to road intersections and whose edges E correspond to road segments. Edge weights W^t are assumed to indicate dynamic traffic conditions (i.e., average speeds, travel time, ...) on the corresponding road segments and are supposed to be known according to a given frequency, e.g., every 30 minutes. Therefore, t represents the time step associated to the observed weights, i.e., the average speeds on the network edges in the analyzed time period. By studying the characteristics of such a dynamic network under both regular conditions and in presence of disruption, via a travel-time dependent weighted graph, we ensure that the proposed combination of dynamic, weighted network indicators is sensitive to perturbations and can be effectively exploited to characterize and, prospectively, predict resilience properties of large-scale networks. In order to perform our analysis and retrieve edge weights, we rely on a real dataset of probe data, as described in Sec. 3.4.1.

3.1. Graph weighting procedure

To introduce the traffic dynamics in the weighted degree centrality (Fig. 1a) computation, with the aim of merging topological and dynamic approaches, the first step consists in obtaining a graph whose weights describe how effectively the edge connects nodes by taking into account actual traffic conditions. We assume that in free flow conditions, all nodes are connected at the best possible level, i.e., all edges have a weight equal to one. When travel time increases, we assume edge weight progressively decreases to zero, with zero corresponding to the case of a completely congested edge, i.e., a road segment where vehicles are completely stuck. By considering the principle of bounded rationality for modelling drivers' behaviors [38, 39], we assume that a small travel time increase should produce a negligible impact on the edge weight (Fig. 1b).Finally, we adopt a discretization process in order to improve the relevance of the edge weights. With this method, only significant travel time variations can actually impact the ability of an edge to connect nodes.

3.2. Degree centrality distribution shifting

As a consequence of the assumption described in the previous section, a travel time increase (caused by congestion phenomena or perturbations) on one edge will imply a reduction in adjacent nodes' weighted degree centrality (Fig. 1a). By generalizing such reasoning to the whole network, we suppose that in presence of a disturbance, the degree distribution is shifted toward the zero value.

This phenomenon is amplified with the disruption intensity and, particularly, in the case of low-resilient networks. On the contrary, when the offset towards zero of the degree distribution is negligible in presence of major disruption affecting the whole network, we can assume the network has higher resilience, by being able to maintain a good level of connection among its nodes.

However, it is worth nothing that, in presence of localized disturbances, the shifting of the degree distributions towards zero could be weak at a global scale (i.e., the whole network), whereas some local areas could be nonetheless strongly impacted. Hence the interest to locally studying the degree distribution to analyze the resilience of the different areas of the network. To that purpose, we always extract the degree centrality values over the whole network to take into account actual traffic dynamics and to preserve network connectivity. However, we analyze and compare both the degree distribution at network scale (i.e., all nodes) and the distribution of the centrality values for a subset of nodes localized around the area mostly impacted by the perturbation. To quantify the offset in degree distributions, we compute the curves of the average degrees over time under normal conditions and in presence of disturbance. Then, we measure the area between the curves.As for the degree distribution offset, the gap between the curves depends on the network resilience and the disruption intensity.

3.3. Heterogeneity analysis

Besides characterizing the impact of perturbations via the degree distribution shifting, we globally study network resilience by measuring its heterogeneity (Eq. 1), density (Eq. 2) and symmetry (Eq. 3) properties. In that sense, we follow an approach similar to the one proposed by Gao et al. [8] to determine the resilience of ecological networks. Based on the weighted in- and out-degree centralities, these measures become sensitive to the traffic conditions. A spatio-temporal analysis, lead by first computing the metrics per areas and then observing their evolution in time, provides interesting insights on the network characteristics and performances. Such analysis allows to have a deep understanding of the network behavior. The comparison of the measures computed under both normal and disrupted conditions is realized in time or at a given time step, for the whole network or by focusing on different areas. Like for the degree distribution shifting analysis, for this spatial analysis, we compute the weighted degree centrality over the whole graph and then extract the degree values of the nodes surrounding the area interested by the perturbation.

3.4. Implementation of the methodology

3.4.1. Generation of a dynamic, weighted graph via probe data

In order to obtain a graph-based representation properly grasping traffic conditions, we build a weighted graph including average travel time information computed from probe data. These data have been recorded during one year, from October 2017 to September 2018, in the Rhônes-Alpes region, France, by a leading provider of real-time traffic and mobility information services[2].

The GPS positions of tracked vehicles have been map-matched to the road network of the Rhônes-Alpes French's region. We have also reduced the area of interest to the Lyon Metropolitan area, so as to conserve a reasonable size and guaranteeing a large availability of speed information on the retained edges. This network is divided in 21 areas, corresponding to the Lyon's districts and neighboring cities (Fig 1d). Afterwards, in order to produce a topologically reliable graph, we have pre-processed it by filtering artificial nodes, thus only retaining those that represent actual road intersections[3]. This step is essential because of the high dependency of the degree centrality to the network topology. With this methodology, we reduced the size of the original graph from

[2] http://www.mediamobile.com/

[3] To obtain the desired graph, we use the Osmnx's Python library [40] which proposes a function that simplifies a city's graph topology by removing all nodes that are not real intersections, entries or exits points of the road network.

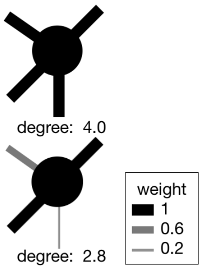

(a) Weighted degree

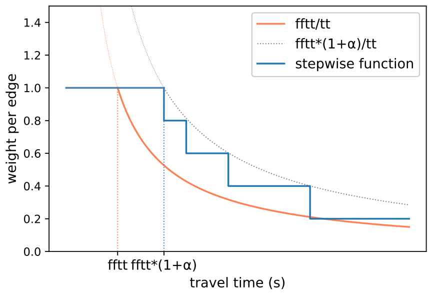

(b) Weight distribution

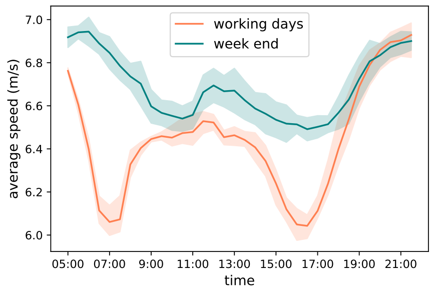

(c) Speed evolution (m/s)

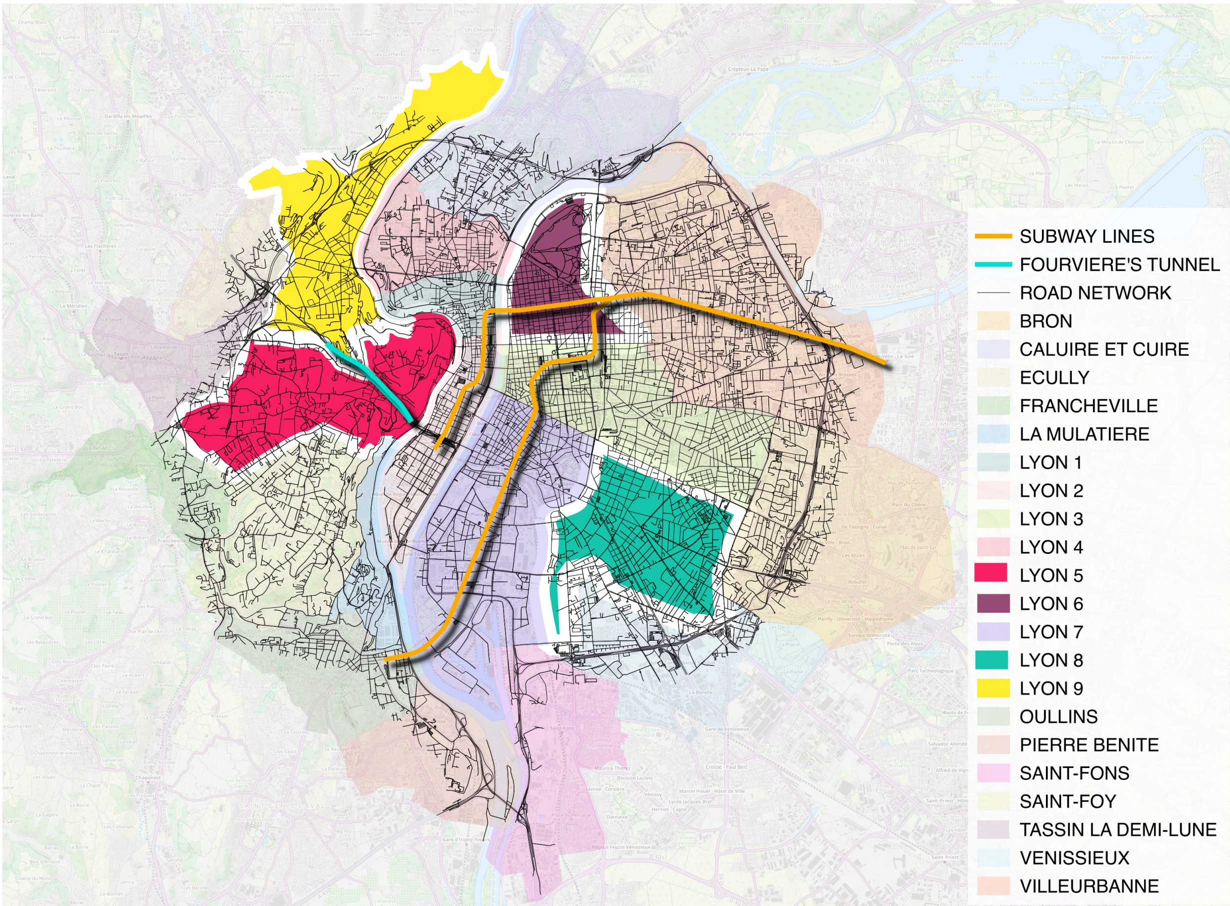

(d) Road network

Figure 1: (a) Computation of a node's unweighted (top) and weighted (bottom) degree centrality. (b) Attribution of a weight to an edge based on observed travel time (in a given time slot) and free-flow travel time. (c) The average speed profile for working days and during the week end. (d) The studied road network of Lyon. The Fourvière's tunnel, closed on the 2^{nd} of June 2018 is highlighted in blue and the disturbed subway lines on the 19^{th} of December 2018 are colored in orange.

21,338 nodes and 39,823 edges to 13,090 nodes and 27,618 edges, coded in Python by using the NetworkX library[4] [41] (Fig. 1d).

In order to produce the average speed with a given periodicity, we aggregate the available speed raw data in 30-minutes slots. The choice of 30 minutes is the result of a sensitivity analysis (not reported due to space limitations), which indicated this value as a preferable choice to obtain a sufficiently large portion of observed edges with a large number of speed samples from the data.

We also analyzed our data to identify both typical and unusual situations of the network in order to understand the sensitivity of the proposed resilience indicators to perturbations. Firstly, we extract the "regular" speed profile, obtained by averaging data over twenty days, for all the edges of the network from 5:00am to 10:00pm which are not interested by any special event or perturbation. Secondly, we obtain unusual speed profiles issued from different specific days presenting a disruption. To do so, we identified specific events, by relying on information recorded from national weather and TMC (Traffic Management Centers), that took place in the observed region and which certainly affected traffic conditions.

As the number of observed vehicles in the probe data is limited, we were not able to always identify speed information for all network edges. Therefore, for those edges where travel time information (either in the case of typical or for abnormal days) were missing, we adopt the simplifying assumptions of free flow conditions, as estimated from the probe data. The data issued from abnormal day are in average available for 35% of the 27,618 edges. This percentage is naturally higher for the typical day, as it has been created by averaging multiple days and related speed observations. Based on the computed speeds (either in regular or unusual conditions) and road segment lengths, we obtain travel time information in each of the above cases.

3.4.2. Studied disruptions

We consider four different disruptions recorded during the period in which data are available. On Monday, December 18th, 2017, the road network was fully disturbed because of a heavy snowfall. On Tuesday, December 19th, 2017, the subway service was blocked from 7:30am to 4:15pm. We analyze the impact of the potential modal shift by studying the change of the road network dynamics. The impact of protesters on the circulation over the road network is analyzed on Wednesday, April 4th, 2018. Finally, on Saturday, June 2nd, 2018, an important tunnel of the city, the "Fourviere's" tunnel, crossed by more than 100,000 vehicles per day, was closed in the north-south direction for renovations during three days. The impact of this localized disturbance is studied at both global and local scales. Some of these disruptions, like the snowfall, affected the whole network whereas some others, like the tunnel closure, are localized in specific zones of the city. For local studies, we deal with these two specific days (December 18th and June 2nd) impact over the 5^{th}, the 6^{th}, the 8^{th} and the 9^{th} districts of Lyon.

3.4.3. Graph weighting procedure

We use a weight discretization process in order to consider a group of edges equivalent when traffic conditions (travel time) are similar, but not necessarily equal. We assume that a travel time increase less than a free flow travel time fraction (i.e., $\alpha.fftt$) has no impact on drivers' route choice decisions. We choose as a proportion $\alpha = 0.2$, knowing the longer per-edge free flow travel time is of 12 minutes. In this case, a travel time of 14.4 minutes ($(1+\alpha).fftt$) is considered as recorded in free flow conditions. In other words, the edge weight is assumed to stay unchanged (and at its highest possible value of 1) for an observed travel time in the range $[0, fftt + \alpha.fftt]$ (Fig. 1b). Beyond this limit, we impose a progressive, decrease of the weight value on the edge, as a step-wise

[4] https://networkx.github.io/documentation/

hyperbolic function of the observed travel time. On Fig. 1b, the orange curve represents the ratio between the free flow travel time and the observed travel time. The blue curve is the discretized travel-time ratio which considers the drivers' bounded rationality principle. The blue curve is the one used to determine the edge weight in a given time slot. In other words, by the proposed discrete function, we are able to model the level of service on each road link, by also taking into account the impact of the (bounded rational) driver's route choice process. An edge with a larger weight (closer to 1) represents a road segment with close-to-free-flow conditions, while lower-weight edges represent road segments exposed to higher congestion or disruption that are working at a reduced level of service, and less likely preferable alternatives for drivers.

3.4.4. Degree distribution shifting

To characterize the impact of the studied disruptions, we compute the degree distribution and the average degree centrality, at each time step, under normal and disturbed conditions. As we noticed a relatively high variance of the speed profile of different days of the week (transparent margins in Fig. 1c), we choose to compare the speed profile of days with unusual behavior with the typical speed profile of the same day of the week (without main disruptions). In other words, if a disturbance happens on a Monday, we compare the traffic conditions of that day with the ones of a typical (non disrupted) Monday. Then, we quantify the difference between both degree distributions (the typical and the unusual) by computing the area between the corresponding average degree curves. This analysis is performed at both global and local scales, by analyzing the degree distribution shifting for the studied areas.

3.4.5. Heterogeneity analysis

By comparing the values of heterogeneity, density and symmetry in normal and disturbed conditions, at global scale, we aim at characterizing the magnitude of a speed reduction over the network. We conduct both temporal and spatial analysis. Firstly, we perform a temporal analysis by plotting the network characteristics from 5:00am to 9:00pm, every two hours. Secondly, we quantify the local impact of disruptions by computing the metrics through the degree distributions of the nodes included in the studied areas. This local analysis also allows to detect localized events hardly detectable at the global scale, but it also provides information on the resilience of specific sub-networks. As an indicator of the impact of the disruption over the metrics, we compute the Euclidean distance between the points determined by the three measures computed in different situations.

4. RESULTS

4.1. Analysis of the Degree Distribution

In this section, we analyze the impact of specific disruptions on the degree distribution. We choose four disturbed scenarios, previously described (Sec. 3.4.2), with adverse effects on traffic conditions, as exhibited by the average speed profiles (Fig. 2a-2d).

4.1.1. Global scale

First, we focus on the typical average speed represented by the blue curves. We notice a lower typical average speed for the three first scenarios (Fig. 2a-2c) than for the last typical one (Fig. 2d). Whereas the three first typical days are working ones, respectively on Monday, Tuesday and Wednesday, the last one happened on a week-end, specifically on a Saturday with different operating conditions in terms of traffic loads. This explains this difference in typical speed profiles computed under normal conditions. A same trend is noticeable in the degree distributions computed for the speeds of the typical days, displayed in blue (Fig. 2e-2h). Under normal conditions, we

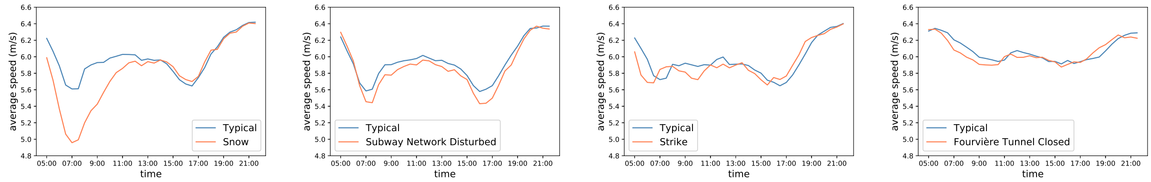

(a) December 18$^{\text{th}}$ (b) December 19$^{\text{th}}$ (c) March 4$^{\text{th}}$ (d) June 2$^{\text{nd}}$

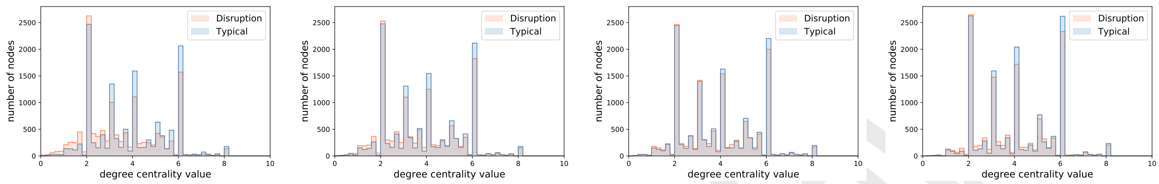

(e) December 18$^{\text{th}}$ (f) December 19$^{\text{th}}$ (g) March 4$^{\text{th}}$ (h) June 2$^{\text{nd}}$

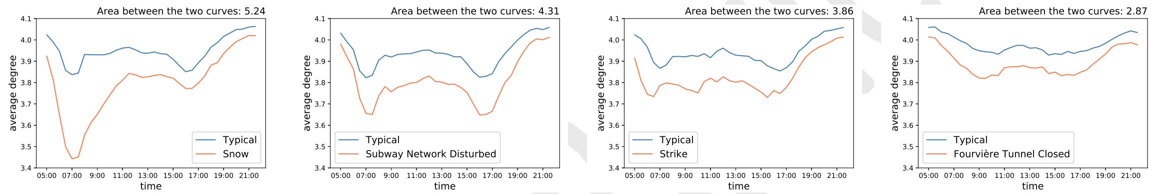

(i) December 18$^{\text{th}}$ (j) December 19$^{\text{th}}$ (k) March 4$^{\text{th}}$ (l) June 2$^{\text{nd}}$

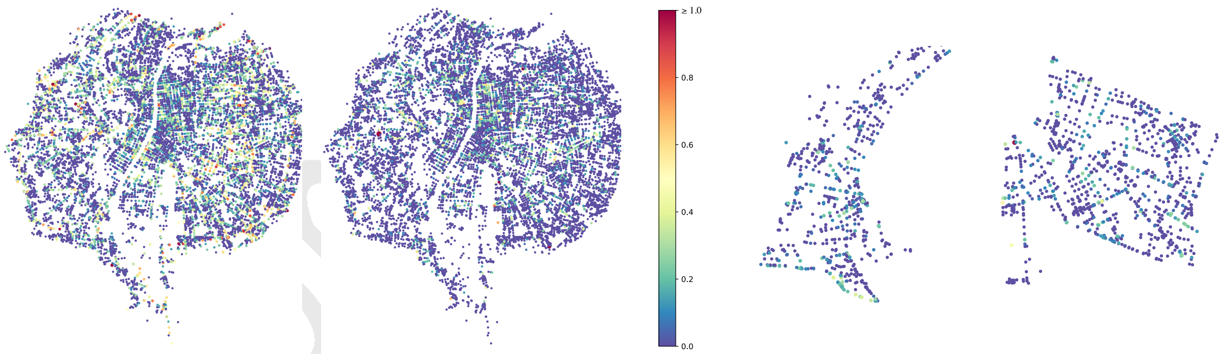

(m) Node loss: December 18$^{\text{th}}$ (n) Node loss: June 2$^{\text{nd}}$ (p) Lyon 5th and 9th (q) Lyon 6th and 8th

Figure 2: The average speed (a)-(d), the degree distribution (e)-(h) and the average degree centrality (i)-(l) are plotted for the four disrupted situations. The degree distribution are computed at 7:30am as the relative error of the degree in typical and disturbed situations observed per node at global scale (m),(n) and by zooming over the impacted (p) or not (q) areas.

notice a larger number of nodes possessing high degree values (between 6.0 and 6.2) for the typical Saturday (Fig. 2h) than for the other days (Fig. 2e-2g). We plotted the degree distributions at 7:30am because we consistently notice a major change between the typical and the observed average speed profiles (Fig. 2a-2d).

For all the studied cases (Fig. 2e-2h), a higher number of nodes, possessing a degree value between 6.0 and 6.2, is observed for the typical distribution than for the disrupted one. This observation is true for the intervals with high degree values. On the contrary, for the ranges grouping small degree values, lower than 3.0, the trend is reversed: there is a larger number of nodes for such degree values in the deteriorated situation than in the normal one. In the presence of disruptions, the degree distributions are shifted to the left, i.e., towards zero. This aspect is exacerbated for the first disruption (Fig. 2e), presenting the most relevant impact on the average speed profile (Fig. 2a).

The comparison of the gap between the two curves, representing the averaged degree centralities, corroborates the impression. Whereas the area between the curves is equal to 5.24 for the first disruption (Fig. 2i), for the second one it is only equal to 4.31 (Fig. 2j). In any events, when computed in disrupted conditions, the average degree is always lower than the one measured under normal conditions (Fig. 2k and 2l). Because of the consideration of the bounded rationality in the graph weighting (Sec. 3.1), the variations in the average degree centrality are higher than for the average speed.

Finally, the computation of the relative error between the weighted degree centralities (Fig. 2m and 2n), issued from typical speeds and abnormal ones, provides information about the localization of the disturbance impact at 7:30am. We notice a stronger impact for the snowfall impact than for the tunnel closure. There a more nodes with a high relative error values for Monday, December 18$^{\text{th}}$ (Fig. 2m), where non-zero values are more dispersed on the network, than for Saturday, June 2$^{\text{nd}}$ (Fig. 2n). By zooming on the studied areas on June 2$^{\text{nd}}$, we notice a higher proportion of nodes with a deteriorated level of service in the districts close to the tunnel than for the other studied ones. In Lyon 5^{th} and Lyon 9^{th} (Fig. 2p), 44% of nodes have a lower level of service with the tunnel closure, against 26% of nodes in Lyon 6^{th} and Lyon 8^{th} (Fig. 2q).

4.1.2. Local scale

We focus now on the impact of the tunnel closure and the snowfall at local scale by observing the behavior of the network locally. We focus on four areas: Lyon 5^{th} and Lyon 9^{th}, localized around the Fourvière's tunnel, more likely to be disturbed, and Lyon 6^{th} and Lyon 8^{th} farther from the tunnel.

First, one can notice a stronger change in the degree distribution for the districts including and surrounding the tunnel (Fig. 3e and 3f). The decrease of the number of nodes with degree centrality value between 6.0 and 6.2 is more important for these areas than for the two other ones (Fig. 3g and 3h). The average degree centrality gap, assessed in computing the area between the curves, confirms the observation. We notice a greater reduction in the average degree centrality for Lyon 5^{th} and 9^{th}, with an area between the two curves respectively equal to 5.56 and 6.57 (Fig. 3i and 3j), than for Lyon 6^{th} and 8^{th} (Fig. 3k and 3l). These districts, far from the disruption, present an area separating the two curves around 3.50. These observations are in accordance with the respective average speed evolution (Fig. 3a, 3b, 3c and 3d).

The second scenario strongly impacts the areas. The 6^{th} district of Lyon is the only one which conserves a similar behavior in both conditions (typical and disrupted). The degree distribution is not modified for the highest degree values (Fig. 3w). Compared to the typical situation, the reduction of the degree occurrence only happens between 3.0 and 4.2. Such an offset has a limited impact on the average degree centrality. Here also, the degree distributions and the average degree conclusions, are in accordance with the average speed evolution (Fig. 3m-3p).

The comparison in results between both studied scenarios also provides insights about the road network. We notice a lower proportion of node with high degree values (between 6.0 and 6.2) in Lyon 5^{th} during the typical Monday than during the typical Saturday. A similar trend is observed for the 9^{th} and the 8^{th} districts of Lyon, where this phenomenon is amplified. These results are in accordance with the average speed difference between the working days and the week-end (Fig. 1c, 3a-3d and 3m-3p). Lyon 6^{th} conserves similar degree distributions and similar average degrees

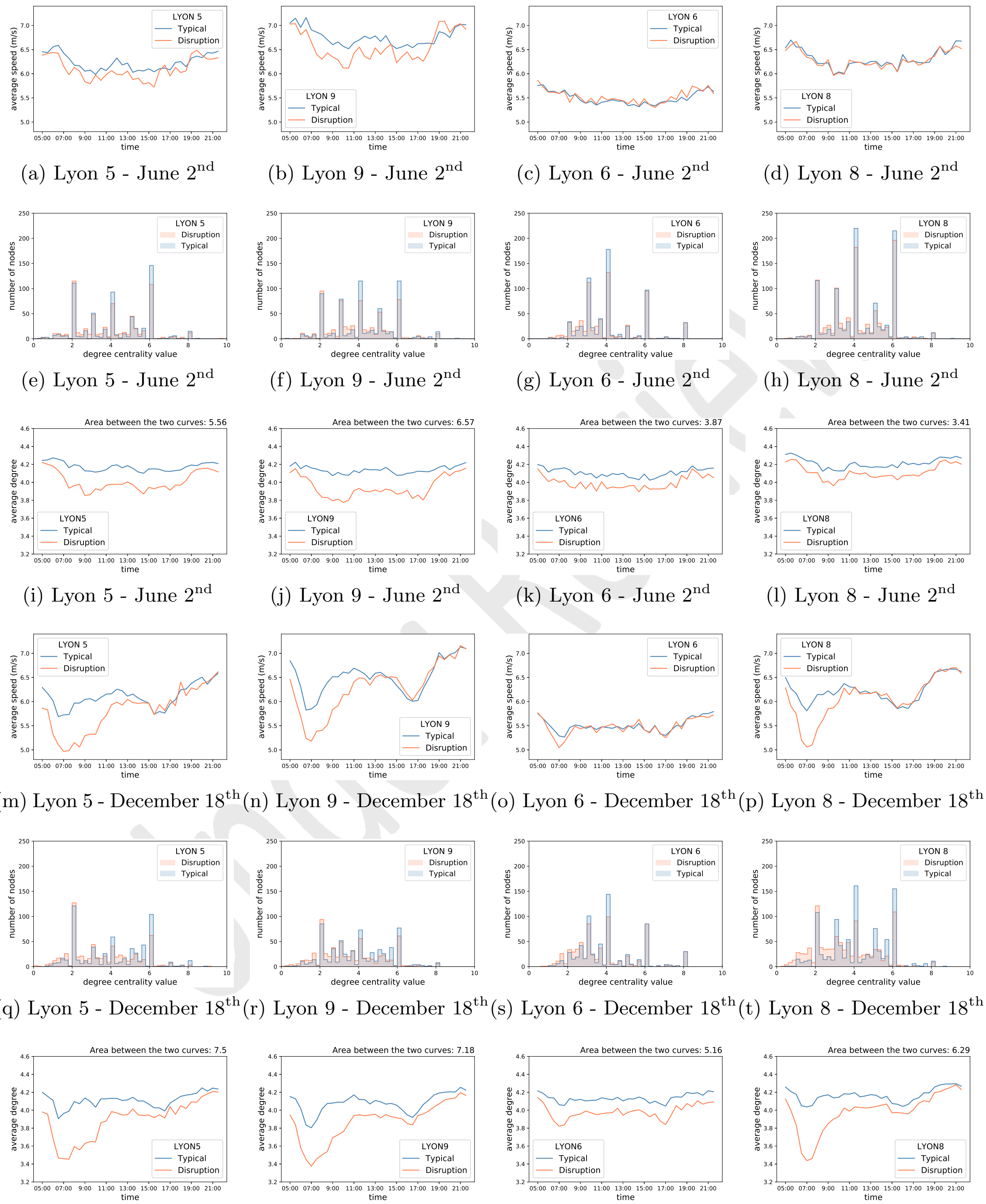

(a) Lyon 5 - June 2$^{\text{nd}}$ (b) Lyon 9 - June 2$^{\text{nd}}$ (c) Lyon 6 - June 2$^{\text{nd}}$ (d) Lyon 8 - June 2$^{\text{nd}}$

(e) Lyon 5 - June 2$^{\text{nd}}$ (f) Lyon 9 - June 2$^{\text{nd}}$ (g) Lyon 6 - June 2$^{\text{nd}}$ (h) Lyon 8 - June 2$^{\text{nd}}$

(i) Lyon 5 - June 2$^{\text{nd}}$ (j) Lyon 9 - June 2$^{\text{nd}}$ (k) Lyon 6 - June 2$^{\text{nd}}$ (l) Lyon 8 - June 2$^{\text{nd}}$

(m) Lyon 5 - December 18$^{\text{th}}$ (n) Lyon 9 - December 18$^{\text{th}}$ (o) Lyon 6 - December 18$^{\text{th}}$ (p) Lyon 8 - December 18$^{\text{th}}$

(q) Lyon 5 - December 18$^{\text{th}}$ (r) Lyon 9 - December 18$^{\text{th}}$ (s) Lyon 6 - December 18$^{\text{th}}$ (t) Lyon 8 - December 18$^{\text{th}}$

(u) Lyon 5 - December 18$^{\text{th}}$ (v) Lyon 9 - December 18$^{\text{th}}$ (w) Lyon 6 - December 18$^{\text{th}}$ (x) Lyon 8 - December 18$^{\text{th}}$

Figure 3: The average speed, the degree distribution and the average degree are plotted for the north-south direction tunnel closure(a)-(l) and the snowfall (m)-(x) for different districts: 5^{th}, 6^{th}, 8^{th} and 9^{th} districts of Lyon. The degree distributions (e)-(h) and (q)-(t) are computed at 7:30am.

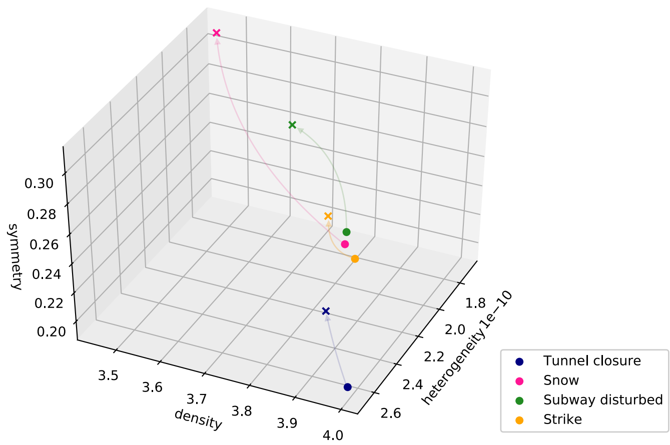

(a) Several disruptions at 7:30am

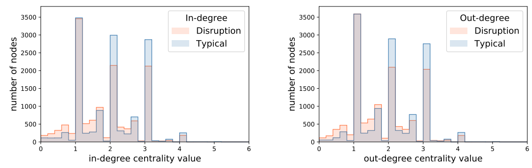

(b) Evolution of in-degree and out-degree in presence or not of snow (18/12/2017) at 7:30am

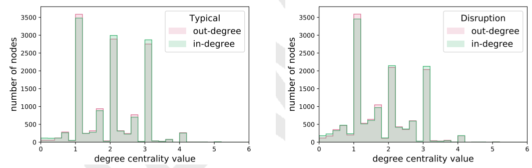

(c) Overlay of in-degree and out-degree in presence or not of snow (18/12/2017) at 7:30am

Figure 4: The heterogeneity, the symmetry and the network density for the global network are plotted under normal conditions (•) and in presence of disruptions (×) in (a) at 7:30am. The distributions in (b) correspond to the in- and out-degree ones under normal condition and in presence of the snowfall at 7:30am. The other distributions superimposed the in- and out-degree in a typical situation (c) and in the presence of the snowfall (d) at 7:30am.

in both studied scenarios, although the area between the curves is a bit higher with the snowfall than for the Fourvière's tunnel closure. For the other areas, the results traduce an impact over the traffic conditions due to the disruptions. Regarding our assumption, the 6^{th} district of Lyon is the most resilient one. This could be explained by a lower typical average speed. Consequently, the gap with the average speed in presence of disruption will be smaller.

4.2. Analysis of the heterogeneity

Having studied the weighted degree centrality behaviors, we focus on the previously presented metrics (Eq. 1, 2 and 3) although the network density, i.e. the average degree, had already been under considerations. The combination of the three indicators will allow us to characterize the network state under different traffic conditions in a spatio-temporal way [8].

4.2.1. Global analysis

For the spatial analysis, all the metrics are computed at 7:30am, where the impacts of the disruptions are the strongest one regarding the average speed profiles (Fig. 1c).

In the presence of the disruption (×), the graph density and its heterogeneity decrease whereas the symmetry grows comparing to the reference situations (•). In Sec. 4.1, we notice the degree distribution shifting toward zero inducing the reduction of the network density (Fig. 3). Therefore, the decline in heterogeneity (Eq. 1) is due to the diminution of the standard deviation of the in-degree and out-degree distributions. The rise of the symmetry value reflects an increase in in-degree and out-degree correlation coefficient. When a disruption occurs, both in-degree and out-degree distributions move to zero, diminishing the corresponding average degrees. Nonetheless, this reduction is accompanied by a stronger decrease of the distribution's standard deviation, hence the increase of the symmetry. The Fig. 4b illustrates the difference of the in-degree (left) and out-

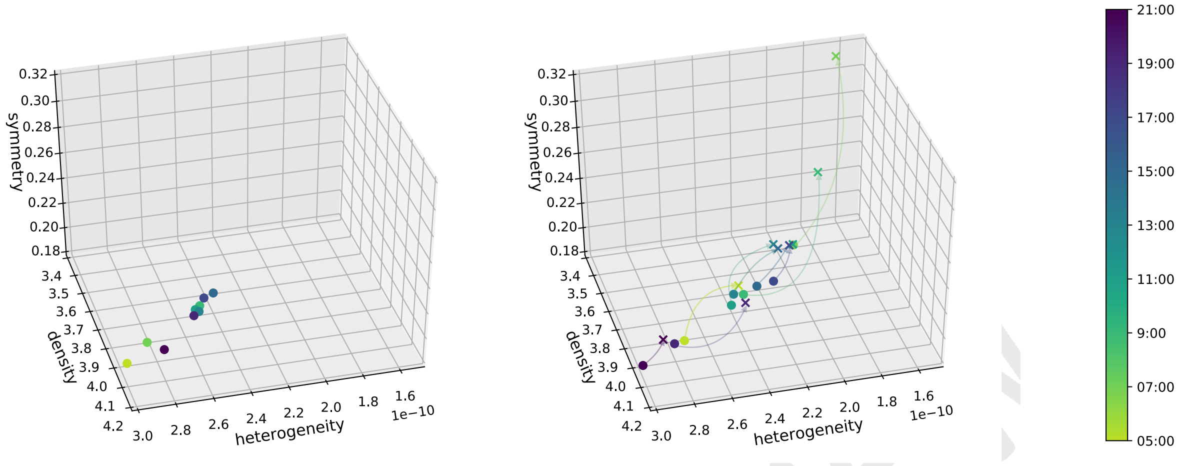

(a) June 2nd (b) December 18th

Figure 5: The heterogeneity, the symmetry and the network density of the global network are plotted under normal conditions on typical Saturday (a) and on typical Monday (b) (•) and in presence of the snowfall (×) in (b) each two hours, from 5:00am to 9:00pm.

degree (right) under normal or abnormal conditions. The Fig. 4c shows a better overlay between the in-degree and the out-degree without disruption (left) or with (right). The correlation coefficient is thus higher in this second case.

The evolution of these three topological indicators, dependent of the traffic dynamics, provides information about the traffic conditions. The lower the value of density and heterogeneity the higher the value of symmetry, with worse traffic conditions.

The impact of the disruptions (×) differs in intensity. The effect of the snowfall is stronger than all others: the corresponding cross and point are the furthest ones with an Euclidean distance of 0.40. This assumption is confirmed by the average speed evolution (Fig. 1c) and the degree shifting (Fig. 2) which present the largest variations for such disruption. On the contrary, the smaller incidence is the one induced by the protesters, with a distance between the reference and the disrupted situations equal to 0.09. The disruption of the subway network and the tunnel closure present moderate impacts with Euclidean distances respectively equal to 0.19 and 0.12.

By comparing the four reference situations (•), computed over typical days, we notice a huge difference between the one corresponding to the tunnel closure and the other disruptions. Whereas the first disturbance occurs on a Saturday, all others happen during week days where typical travel time are lower (Fig. 1c), explaining the difference in network states.

4.2.2. Global scale - Temporal analysis

Due to the traffic conditions, we expect a time-dependent evolution of the network state as a time-dependent impact of the disruptions. To explore these aspects, we plot the indicators for the typical Saturday (Fig. 5a) and the typical Monday and the one disturbed by the snowfall (Fig. 5b) from 5:00am to 9:00pm, each two hours for the sake of readability.

By leveraging a dynamic graph, we are able to characterize the time-dependent network state through the three indicators. In both situations, corresponding to a typical Saturday (Fig. 5a) and a typical Monday (Fig. 5b), the heterogeneity and the density are the highest one with the smallest

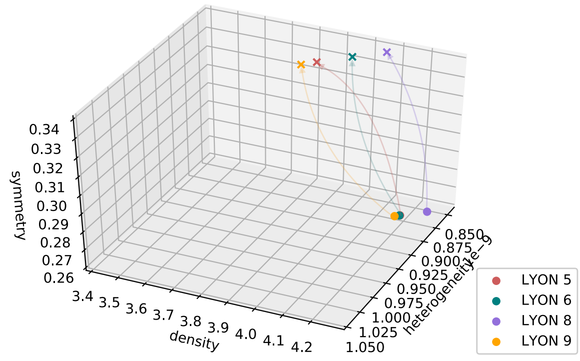

(a) June 2$^{\text{nd}}$ at 7:30am

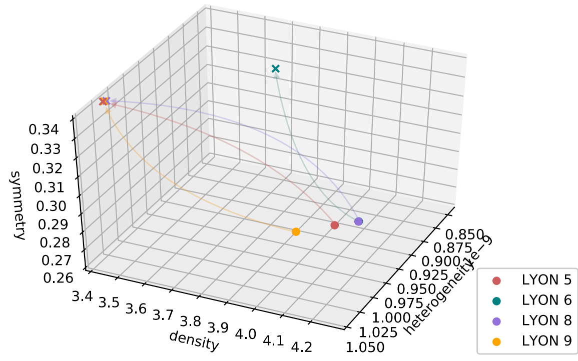

(b) December 18$^{\text{th}}$ at 7:30am

Figure 6: The local heterogeneity, the local symmetry and the local network density, are plotted under normal conditions (•) and in presence of the tunnel closure (×) in (a) and the snowfall (×) in (b) at 7:30am for four districts.

symmetry value for extreme hours (5:00am and 9:00pm), when the traffic conditions are better than during the day. Regarding the typical Saturday (Fig. 5a), there is also good traffic conditions at 7:00am, regarding the position of the corresponding point in the 3D-map. This statement is confirmed by the week-end speed with the translation of the first reduction from 7:00am to 9:00am (Fig. 1c). On the contrary, on a typical Monday (Fig. 5b) we have the worst traffic conditions at 7:00am due to the morning peak-hour. Nonetheless, we have good traffic conditions at 7:00pm, in accordance with the speed profile of the working days (Fig. 1c).

In Fig. 5b, we plot the network state when disrupted by the snowfall. The highest change between the typical situation and the disrupted one happens at 7:00am and 9:00am (Fig. 5b), in accordance with the evolution of the speed profile (Fig. 2a).

4.2.3. Local scale - Spatial analysis

To lead the spatial analysis, the metrics are computed for the four studied districts at the same time, 7:30am. The Fig. 6a presents the network density, heterogeneity and symmetry on Saturday, June 2$^{\text{nd}}$, 2018 when the north-south direction of the Fourvière's tunnel was closed. The Fig. 6b illustrates the same metrics for the same districts impacted by a snowfall on December 18$^{\text{th}}$.

The impact over the 5^{th} and 9^{th} districts is stronger for the tunnel closure (Fig. 6a) than for the two other areas. Indeed, the Euclidean distance between the point and the corresponding cross for the 5^{th} and 9^{th} districts of Lyon are respectively equal to 0.25 and 0.29, against 0.17 for the 6^{th} district and 0.16 for the 8^{th} one. This trend was already observed with the average speed profiles evolution (Fig. 3a,3c, 3d and 3b) and the degree shifting (Fig. 3e,3g, 3h and 3f). Regarding the second disrupted situation (Fig. 6b), the districts are similarly impacted, expect the 6^{th} one. We already observed this specific behavior with the degree distribution translation analysis (Fig. 3o, 3s and 3w). In any scenarios, the Euclidean distances between reference situations and disrupted ones are larger for the snowfall than for the tunnel closure: respectively 0.54, 0.23, 0.60 and 0.44 for the 5^{th}, the 6^{th}, the 8^{th} and the 9^{th} districts.

We notice a different behavior for the areas in terms of resilience. The network states, characterizing by the heterogeneity, the density and the symmetry, are close, even superimposed, for the 6^{th} and the 8^{th} districts for the typical Monday whereas in presence of the snowfall affecting both areas (Fig. 6b), their corresponding parameter are far from each other.

On the typical Saturday, the 8^{th} district has a different behavior under normal conditions (Fig. 6a. This could be explained by the higher number of nodes. Moreover, in this area, there is a large amount of high degree value. This could be caused by (i) a better topological node connection or (ii) a higher amount of nodes presenting free flow conditions. By computing the topological average degree, we are able to affirm we are in the second case. Indeed, the average topological degree is higher for the 6^{th} district than for the 8^{th} one. The degree distribution observed for the typical Saturday (Fig. 3d) also shows this distinction by presenting a higher number of nodes with a large value than in other areas. Regarding the other districts (Fig. 6a), the 9^{th} one has a typical behavior close to the 5^{th} and the 6^{th} ones with a similar average speed profile (Fig. 3a-3c). The trend changes during the working day (Fig. 6b), where the area average speed profile is higher for 9^{th} district than the two other ones (Fig. 3m-3o).

5. CONCLUSION AND PERSPECTIVES

With this work, we contribute to the network resilience analysis by studying the impact of disruptions on resilience through the degree centrality and other global metrics based on the network characteristics. By considering static and dynamic resilience aspects, we are able to quantify the resilience considering the topological vulnerabilities and the traffic conditions.

The translation of the degree distribution (Sec. 4.1) evolution has proved to be sensitive to disruptions, confirming our initial assumption. This change in degree implies a modification in heterogeneity, density and symmetry used to compute the network state in the 3D-figure as performed in [8] (Sec. 4.2). We notice the reduction in heterogeneity and density, associated with the increase of the symmetry is due to the presence of disruptions. The more the impact is intense, the higher this behavior is amplified. Thus, these metrics are interesting in resilience analysis by well-grabbing traffic conditions on the network state.

For future works, we plan to work on the critical value of the macroscopic resilience indicator [8]. With such information, the plan between the resilient and the non-resilient phases can be determined and plotted on the three-dimensional figures (Fig. 4a, 5 and 6).

With probe data, we do not have access to all the per-edge travel time per day. Although we observe an impact of disruptions over the traffic conditions, by replacing the unknown values with the typical ones, we mitigate the impact of the disruption in our results. By leading this methodology with simulated data rather than real ones, we could have all the travel time and we are able to stress the network in the way we want. This study would be essential to better characterize the area resilience by applying specific disruptions over the network and quantifying such impact in metrics computed with synthetic data.

With such analysis we could be able to characterize the resilience of multimodal transport network which one of our objectives. The degree centrality is as a matter of fact easily computable over a multi-layer graph. Therefore, the presented methodology is easily convertible for such network which could present different resilience characteristics. The impact of a disturbance of a unique transport mode could be compensated by a modal shift.

ACKNOWLEDGMENT
This work has been supported by the French ANR research project PROMENADE, grant number ANR-18-CE22-0008.

The authors confirm contribution to the paper as follows: study conception and design: E. Henry, A. Furno, N.-E. El Faouzi; data collection: E. Henry, A. Furno, N.-E. El Faouzi; analysis and interpretation of results: E. Henry, A. Furno, N.-E. El Faouzi; draft manuscript preparation: E. Henry, A. Furno, N.-E. El Faouzi. All authors reviewed the results and approved the final version of the manuscript.

References

[1] Amer Shalaby, P Eng, and David King. Performance Metrics and Analysis of Transit Network Resilience in Toronto. *Transport Research Board*, 2016.

[2] Xiaodong Zhang, Elise Miller-Hooks, and Kevin Denny. Assessing the role of network topology in transportation network resilience. *Journal of Transport Geography*, 46:35–45, 6 2015.

[3] Yew-Yih Cheng, Roy Ka, Wei Lee, Ee-Peng Lim, and Feida Zhu. Measuring Centralities for Transportation Networks Beyond Structures. *Lecture Notes in Social Networks*, 2015.

[4] Pamela Murray-Tuite. A comparison of transportation network resilience under simulated System Optimum and User Equilibrium conditions. *Proceedings of the 2006 Winter Simulation Conference*, 2006.

[5] Erik Jenelius, Tom Petersen, and Lars-Göran Mattsson. Importance and exposure in road network vulnerability analysis. *Transportation Research Part A*, pages 537–560, 2006.

[6] Pauline Gauthier, Angelo Furno, and Nour-Eddin El Faouzi. Road network resilience: how to identify critical linkssubject to day-to-day disruptions? *Transport Research Record*, 2018.

[7] Elise Henry, Angelo Furno, and Nour-Eddin El Faouzi. A Graph-based Approach with Simulated Traffic Dynamics 1 for the Analysis of Transportation Resilience in Smart Cities. In *Transport Research Board 98th Annual Meeting*, Washington DC, 2019.

[8] Jianxi Gao, Baruch Barzel, and Albert László Barabási. Universal resilience patterns in complex networks. *Nature*, 2016.

[9] B Berche, C Von Ferber, T Holovatch, and Yu Holovatch. Resilience of public transport networks against attacks. *Eur. Phys. J. B*, 71:125–137, 2009.

[10] Grant Silver, Meisam Akbarzadeh, and Ernesto Estrada. Tuned communicability metrics in networks. The case of alternative routes for urban traffic. *Chaos, Solitons & Fractals*, 116:402–413, 11 2018.

[11] Jan Scheurer, Carey Curtis, and Sergio Porta. Spatial Network Analysis of Public Transport Systems: Developing a Strategic Planning Tool to Assess the Congruence of Movement and Urban Structure in Australian Cities. In *30th Australasian Transport Research Forum (ATRF*, 2007.

[12] Vito Latora and Massimo Marchiori. Efficient Behavior of Small-World Networks. *Physic Review*, 87(89), 2001.

[13] Michal Bíl, Rostislav Vodák, Jan Kubeček, Martina Bílová, and Jiří Sedoník. Evaluating road network damage caused by natural disasters in the Czech Republic between 1997 and 2010. *Transportation Research Part A: Policy and Practice*, 80:90–103, 10 2015.

[14] Nazli Yonca Aydin, Hans Rudolf Heinimann, H Sebmen Duzgun, and Friedemann Wenzel. Integration of stress testing with graph theory to assess the resilience of urban road networks under seismic hazards. *Natural Hazards*, 91:37–68, 2018.

[15] Huijuan Wang, Javier Martin Hernandez, and Piet Van Mieghem. Betweenness centrality in a weighted network. *Physical Review E - Statistical, Nonlinear, and Soft Matter Physics*, 2008.

[16] Meisam Akbarzadeh, Soroush Memarmontazerin, Sybil Derrible, and Sayed Farzin Salehi Reihani. The role of travel demand and network centrality on the connectivity and resilience of an urban street system. *Transportation*, pages 1–15, 8 2017.

[17] Yaniv Altshuler, Rami Puzis, Yuval Elovici, Shlomo Bekhor, and Alex Pentland. Augmented Betweenness Centrality for Mobility Prediction in Transportation Networks. 2011.

[18] Aisan Kazerani and Stephan Winter. Can Betweenness Centrality Explain Traffic Flow? Technical report.

[19] Ian X. Y. Leung, Shu-Yan Chan, Pan Hui, and Pietro Lio'. Intra-City Urban Network and Traffic Flow Analysis from GPS Mobility Trace. 2011.

[20] K P Harikrishnan, Rinku Jacob, R Misra, and G Ambika. Measure for degree heterogeneity in complex networks and its application to recurrence network analysis.

[21] A Barrat, M Barthé Lemy †, R Pastor-Satorras, and A Vespignani. The architecture of complex weighted networks. Technical report, 2004.

[22] M E J Newman. Analysis of weighted networks.

[23] Tore Opsahl, Vittoria Colizza, Pietro Panzarasa, and José J Ramasco. Prominence and Control: The Weighted Rich-Club Effect. *To PRL*, 101:168702, 2008.

[24] Tore Opsahl, Filip Agneessens, and John Skvoretz. Node Centrality in Weighted Networks: Generalizing Degree and Shortest Paths. Technical report.

[25] Luca Dall'Asta, Alain Barrat, Marc Barthélemy, and Alessandro Vespignani. Vulnerability of weighted networks. *Journal of Statistical Mechanics: Theory and Experiment*, (4), 4 2006.

[26] Tom A. B. Snijders. The degree variance: an index of graph heterogeneity. *Social Networks*, 1981.

[27] Martín G Zimmermann, Víctor M Eguíluz, and Maxi San Miguel. Coevolution of dynamical states and interactions in dynamic networks.

[28] Keith Smith and Javier Escudero. Normalised degree variance: a network heterogeneity index unbiased to size and density. Technical report.

[29] Lothar Von Collatz and Ulrich Sinogowitz. Spektren endlicher grafen. *Abhandlungen aus dem Mathematischen Seminar der Universität Hamburg*, 21(1):63–77, 12 1957.

[30] M.O. Albertson. The irregularity of a graph. *Ars Combinatoria*, 1997.

[31] Ernesto Estrada. Quantifying network heterogeneity. 2010.

[32] Shumaila Yousaf, Akhlaq Ahmad Bhatti, and Akbar Ali. A Note on the Modified Albertson Index. Technical report, 2019.

[33] Ginestra Bianconi. The entropy of network ensembles. Technical report, 2008.

[34] Pavlos Tamvakis and Yiannis Xenidis. Comparative Evaluation of Resilience Quantification Methods for Infrastructure Systems. *Procedia - Social and Behavioral Sciences*, 2013.

[35] Rawia Ahmed El-Rashidy and Susan Grant-Muller. The evaluation of redundancy for road traffic networks. *TRANSPORT*, 2016.

[36] Bing Wang, Huanwen Tang, Chonghui Guo, and Zhilong Xiu. Entropy optimization of scale-free networks' robustness to random failures. *Physica A: Statistical Mechanics and its Applications*, 363(2):591–596, 5 2006.

[37] Leonor Michaelis and Maud Leonora Menten. Fundamentals of Enzyme Kinetics : Michaelis-Menten and Deviations.

[38] Gerd Gigerenzer and Reinhard Selten. *Bounded rationality : the adaptive toolbox*. MIT Press, 2001.

[39] Michael Sivak. How common sense fails us on the road: contribution of bounded rationality to the annual worldwide toll of one million traffic fatalities. *Transportation Research Part F: Traffic Psychology and Behaviour*, 5(4):259–269, 2002.

[40] Geoff Boeing. OSMnx: New methods for acquiring, constructing, analyzing, and visualizing complex street networks. *Computers, Environment and Urban Systems*, 65:126–139, 9 2017.

[41] Aric A. Hagberg, Daniel A. Schult, and Pieter J. Swart. Exploring Network Structure, Dynamics, and Function using NetworkX. In *Proceedings of the 7th Python in Science Conference (SciPy 2008)*, 2008.